

Enhancing Enumeration-Based Model Predictive Control for DC-DC Boost Converter with Event-Triggered Control

Ranya Badawi, *Student Member, IEEE* and Jun Chen, *Senior Member, IEEE*

Abstract—This paper investigates the use of event-triggered model predictive control (MPC) to enhance the performance of an enumeration-based MPC for a DC-DC boost converter. Enumeration-based MPC utilizing a discrete-time switched model has been used to track a converter's output voltage to a given reference. The optimization process of enumeration-based MPC relies on evaluating the cost function for every enumerated sequence, which leads to a great number of computations. For time-triggered MPC, this optimization process is repeated at every control loop. To reduce online computations while maintaining comparable control performance, event-triggered MPC only runs the optimization problem when an event is triggered. The control performance of both time-triggered and event-triggered MPC methods are simulated and compared, with the advantage of using event-triggered MPC being clearly demonstrated.

I. INTRODUCTION

Power converters play a major role in many industries such as automotive, renewable energy, aviation, etc. Their ability to efficiently convert power, boost voltage, reverse polarity and isolate the input from output ground references have placed them at a clear advantage to their linear regulator counterparts. Converter control is needed to track the output voltage despite disturbances in the input voltage and load current. Among many control techniques, linear pulse width modulation (PWM) with PI control and non-linear hysteresis controllers have been extensively analyzed and are well-developed control strategies for power converters [1]. Recently, digital control, such as fuzzy [2] and predictive control, has been gaining popularity as it enables more advanced control techniques. Digital control offers several advantages over analog control such as higher accuracy, flexibility, speed, and lower cost [3].

Recent research has also focused on using model predictive control (MPC) for power converter control [4], [5] and [6]. MPC uses a dynamical model of the system to predict its future behavior given its current state and a set of independent variables over a future time frame called the prediction horizon. For enumeration-based MPC, several predefined control sequences are first assembled. An optimization problem is then formulated to evaluate all predefined control sequences, and the optimal control action is then selected from the one control sequence that minimizes the cost function. Like all moving horizon control techniques,

only the first element of the optimal sequence of control is applied to the actuator. For time-triggered MPC, the above optimization process is repeated at each sample time in a way that the optimization problem is repeated with updated system measurements [4].

Time-triggered MPC has been successfully implemented for DC-DC boost converter control in [4]. However, the disadvantage of this control method is that it requires a microcontroller with substantial computational power to solve the optimization problem at every sample time. This is especially a challenge when controlling switching converters since their switching frequencies are typically in the order of tens and hundreds of kHz. The controller must operate fast enough to solve the optimization problem before the next switching cycle [1]. Furthermore, due to the non-minimum phase behavior from the control input to the output voltage of boost converters, a long prediction horizon is needed, which increases the computational requirement exponentially [4], [7].

To address the computation burden, this paper proposes using an event-triggered control framework for DC-DC boost converter control. More specifically, a similar control problem to that of [4] is considered, where MPC is used as a voltage-mode controller for a DC-DC boost converter to track the output voltage to a reference value, while operating over a wide input range rejecting any disturbance at the input source. Both continuous conduction mode (CCM) as well as discontinuous conduction mode (DCM) are explicitly considered by the dynamical model to improve prediction. To reduce online computations, the optimization problem is formulated and solved only when a triggering event is on. Otherwise, the optimal control sequence from the previous optimization is shifted to determine the current switch input. Therefore, the proposed control strategy substantially differs from [4] which uses time-triggered MPC to solve the optimization problem at every sample time. Simulation results using MATLAB/Simulink clearly demonstrate the saving of computations by up to 93%, while achieving control performance that is comparable to time-triggered formulation. Note that event-triggered MPC has been studied for various applications. See [8]–[15], and reference therein. However, the application of event-triggered enumeration-based MPC for power converter control has not been reported in literature.

The rest of this paper is organized as follows. Section II introduces the model of the DC-DC boost converter, while both time-triggered and event-triggered enumeration-based MPC are presented in Section III. Simulation results are

This work is supported in part by SECS Faculty Startup Fund and URC Faculty Research Fellowship at Oakland University. Jun Chen is the corresponding author.

Ranya Badawi and Jun Chen are with the Department of Electrical and Computer Engineering, Oakland University, Rochester, MI 48309, USA (emails: ranyabadawi@oakland.edu, junchen@oakland.edu).

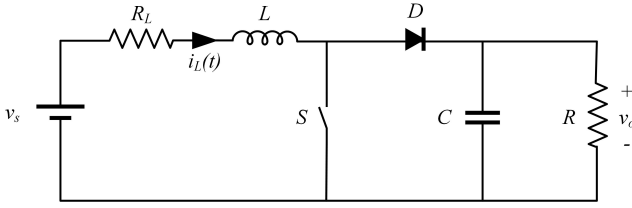


Fig. 1. DC-DC Boost Converter

presented and discussed in Section IV, and the paper is concluded in Section V.

II. BOOST CONVERTER DISCRETE-TIME MODEL

This section briefly introduces the dynamical model of a DC-DC boost converter. For more details, please refer to [4]. The DC-DC boost converter increases the input voltage $v_s(t)$ to a higher DC output voltage $v_o(t)$. A circuit diagram of a typical boost converter is shown in Fig. 1, which can work in three sub-states.

- 1) The first subinterval is when switch S is ON and the inductor current $i_L(t)$ is increasing.
- 2) The second subinterval occurs when switch S is OFF; the inductor current is decreasing and greater than zero.
- 3) The third subinterval represents DCM operation; switch S and diode D are OFF and the inductor current is zero. This third subinterval does not occur in CCM operation.

Let the inductor current and output voltage (capacitor voltage) be the state variables. In other words,

$$x(t) = [i_L(t) \quad v_o(t)]^T \quad (1)$$

During the first subinterval, S is ON, diode D is OFF and the inductor current is increasing linearly. The capacitor is contributing current to the load resistor, R . R_L is the DC resistance of the inductor, L . The circuit is represented with the following state representation:

$$\dot{x}(t) = \begin{bmatrix} -\frac{R_L}{L} & 0 \\ 0 & -\frac{1}{RC} \end{bmatrix} x(t) + \begin{bmatrix} \frac{1}{L} \\ 0 \end{bmatrix} v_s(t) \quad (2a)$$

In the second subinterval, the inductor is connected to the load through the diode. The inductor current is positive and decreasing. During this time, the capacitor is being charged and power is being provided to the load. It is represented by (2b).

$$\dot{x}(t) = \begin{bmatrix} -\frac{R_L}{L} & -\frac{1}{L} \\ \frac{1}{C} & -\frac{1}{RC} \end{bmatrix} x(t) + \begin{bmatrix} \frac{1}{L} \\ 0 \end{bmatrix} v_s(t) \quad (2b)$$

During the third subinterval, both switch S and diode D are OFF and the circuit reduces to the capacitor and load resistance. This operating state is represented by (2c).

$$\dot{x}(t) = \begin{bmatrix} 0 & 0 \\ 0 & -\frac{1}{RC} \end{bmatrix} x(t) + \begin{bmatrix} 0 \\ 0 \end{bmatrix} v_s(t) \quad (2c)$$

The discrete-time model is derived based on the continuous-time model in (2) with the forward Euler approximation approach where T_s is defined as the time step. The converter can operate in four different modes, depending on the shape of the inductor current [4]:

- 1) Mode 1 represents the converter when switch S is ON and the inductor current is increasing.
- 2) Mode 2 is when switch S is OFF and the inductor current is decreasing and is positive.
- 3) Mode 4 is when both switch S and diode D are OFF and the inductor current is 0.
- 4) Mode 3 is the average of Modes 2 and 4 and includes the moment when the inductor current decreases from a positive value and reaches 0, which is defined as τ_1 .

The discrete-time state space matrices for all four modes are included below (3).

Mode 1:

$$x[k+1] = \begin{bmatrix} 1 - \frac{R_L T_s}{L} & 0 \\ 0 & 1 - \frac{T_s}{RC} \end{bmatrix} x[k] + \begin{bmatrix} \frac{T_s}{L} \\ 0 \end{bmatrix} v_s[k] \quad (3a)$$

Mode 2:

$$x[k+1] = \begin{bmatrix} 1 - \frac{R_L T_s}{L} & -\frac{T_s}{L} \\ \frac{T_s}{C} & 1 - \frac{T_s}{RC} \end{bmatrix} x[k] + \begin{bmatrix} \frac{T_s}{L} \\ 0 \end{bmatrix} v_s[k] \quad (3b)$$

Mode 3:

$$x[k+1] = \begin{bmatrix} 1 - \frac{R_L \tau_1}{L} & -\frac{\tau_1}{L} \\ \frac{\tau_1}{C} & 1 - \frac{T_s}{RC} \end{bmatrix} x[k] + \begin{bmatrix} \frac{\tau_1}{L} \\ 0 \end{bmatrix} v_s[k] \quad (3c)$$

Mode 4:

$$x[k+1] = \begin{bmatrix} 1 & 0 \\ 0 & 1 - \frac{T_s}{RC} \end{bmatrix} x[k] \quad (3d)$$

III. MODEL PREDICTIVE CONTROL

We start with a general description of enumeration MPC, followed by proposing event-triggered MPC to reduce online computations.

A. Time-triggered Enumeration-based MPC

For the DC-DC boost converter described above, a set of switching sequences are assembled over the prediction horizon, where the length of horizon is denoted as N . Each switching sequence is in the form $U(k) = [u(k), u(k+1) \dots u(k+N-1)]^T$. To achieve longer prediction, a move

blocking scheme can be implemented, as is done in [4]. Note that the total number of switching sequences is 2^N . The MPC solves an optimal control problem (OCP) for each switching sequence, formulated as follows.

$$\min_{U_o} \sum_{\ell=k}^{k+N-1} (|v_{o,err}(\ell+1|k)| + \lambda|\Delta u(\ell|k)|) \quad (4a)$$

$$\text{s.t. System dynamics (3)} \quad (4b)$$

In other words, the MPC controller predicts the future output of the converter given a switch state within a sequence, the estimated input voltage, inductor current and output voltage at the time step. The absolute voltage error ($v_{o,err}(k) = v_{ref} - v_o(k)$) and difference in switch state ($\Delta u(k) = u(k) - u(k-1)$) are then calculated for each switch state within the sequence. The weighing factor, λ , is applied to the difference between the two consecutive switching states to adjust the amount of switching, where increasing λ generally reduces the switching frequency. At each time step, the MPC controller evaluates the cost function (4) for each of predefined switching sequences $U(k)$. In other words, for each of the 2^N sequences, the output voltage trajectory is predicted, and the objective function is evaluated. The switching sequence with minimum cost function value is then selected as the optimal switching sequence $U_o(k)$. The first element of the sequence is applied to the switch, S . For time-triggered MPC, this procedure is repeated at the next time-step, based on new measurements acquired at the following sampling instance.

B. Event-Triggered Enumeration-based MPC

The enumeration technique considers all possible combinations of the switching states over the prediction horizon. For each of the 2^N sequences, the output voltage trajectory is predicted, and the objective function is evaluated at every time-step. This requires significant computational power, which increases exponentially when the prediction length N is increased. To address this issue, event-triggered MPC is proposed to solve the optimization problem only when an event is triggered, as opposed to solving at every time step. Note that the idea of event-triggered MPC has been studied in [16] and [15], and the adoption to enumeration-based MPC and application to a DC-DC boost converter has not been reported in literature. At the sampling time, given the optimal state sequence X_{t1} computed at the last event (at time t_1), and the current output voltage measurement, v_o , an event e is defined by:

$$e = \begin{cases} 1 & \text{if } ||X_{t1}(2, k) - v_o|| > \delta \text{ or } k > k_{max} \\ 0 & \text{Otherwise} \end{cases} \quad (5)$$

An event is triggered when $e = 1$. In this case, the enumeration based MPC is triggered to solve the optimization problem and returns the optimal control sequence U_t , where $U_t = U_o$. Otherwise, when $e = 0$, the control action is determined using the next switch state in the optimal sequence U_{t1} computed at the last event, thus avoiding running the optimization problem for the 2^N switching

sequences [15]. The event-triggered control algorithm is described in Algorithm 1. The cost function in Algorithm 1 is the argument of the OCP in (4a) and is defined as J . Fig. 2 shows a block diagram of the proposed system.

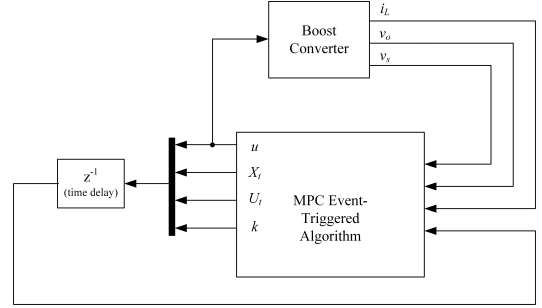


Fig. 2. DC-DC Boost Converter with MPC Control

The proposed event-triggered MPC block will output the entire optimal switching sequence U_t and optimal state trajectory X_t in addition to the actuating switching signal u . We also define index k and output the index from the controller. k is such that sampling time $t = t_1 + kT_s$ where T_s is the sampling time. The optimal switching sequence U_t , optimal state trajectory X_t , the switch state, and index k are sent back to the MPC block as inputs after one time step delay. In the beginning of the MPC block, we increment index k by 1. We then evaluate e from (5) by comparing the sampled state v_o , also defined as $x(2)$, against $X_{t1}(2, k)$ which was computed from the previous time step. If an event is triggered, $e = 1$, index k is reset to 0 and the OCP is calculated with updated optimized state and switching sequences outputted from the controller. If $e = 0$, the actuation will be set to $U_{t1}(k+1)$. The closed loop system consisting of the boost converter and MPC controller were implemented in MATLAB/Simulink and the simulation results are reported in the following section.

IV. SIMULATION RESULTS

Simulation results for both time-triggered and event-triggered control are presented. The performance of the boost converter is evaluated during startup, step change in the input voltage and step changes in voltage reference. The parameters used in all simulations are listed in Table I. In all simulations, $k_{max} = N$, where N is the prediction horizon. The input voltage v_s is set to 10V and the output voltage reference v_{ref} is 15V unless stated otherwise. The threshold δ to determine a triggering event is selected to be 0.05.

A. Start-up

A start-up under normal condition is simulated, with results shown in Figs 3 and 4. For event-triggered MPC, Fig. 4, we additionally plot the event frequency to denote computational savings. Note that for the ease of presentation, the event frequency is averaged using a moving window to show the average triggering frequency. As can be seen from the simulated waveforms, the converter reaches the desired

Algorithm 1 Event-Triggered MPC Algorithm

```

1: procedure ETMPC( $u, U_{t1}, X_{t1}, k, i_L, v_o, v_s$ )
2:    $J^*(k) = \infty$ ;
3:    $k \leftarrow k + 1$ 
4:    $e \leftarrow \text{compute (5)}$ ;
5:   if  $e = 1$  then
6:      $k \leftarrow 0$ 
7:     for all  $U$  over  $N$  do
8:        $J = 0$ 
9:       for  $\ell = k$  to  $k + N - 1$  do
10:         $x(\ell + 1) \leftarrow \text{compute from (3)}$ 
11:         $v_{o,err}(\ell + 1) = v_{ref} - v_o(\ell + 1)$ 
12:         $\Delta u(\ell) = u(\ell) - u(\ell - 1)$ 
13:         $J = J + |v_{o,err}(\ell + 1)| + \lambda |\Delta u(\ell)|$ 
14:       end for
15:       if  $J < J^*(k)$  then
16:          $J^*(k) = J, u = U(1)$ 
17:       end if
18:     end for
19:      $U_t \leftarrow U$ 
20:      $X_t \leftarrow x$ 
21:   else
22:      $u \leftarrow U_{t1}(k + 1)$ 
23:      $U_t \leftarrow U_{t1}$ 
24:      $X_t \leftarrow X_{t1}$ 
25:   end if
26: return  $u, k, U_t, X_t$ 
27: end procedure

```

reference at about 2ms without overshoot using both time-triggered and event-triggered MPC. Initially, the controller keeps switch S open to charge the output capacitor as quickly as possible to the reference voltage. Once the output voltage is within the range of the input voltage, the controller begins to operate, and the converter begins to boost the voltage to the reference voltage.

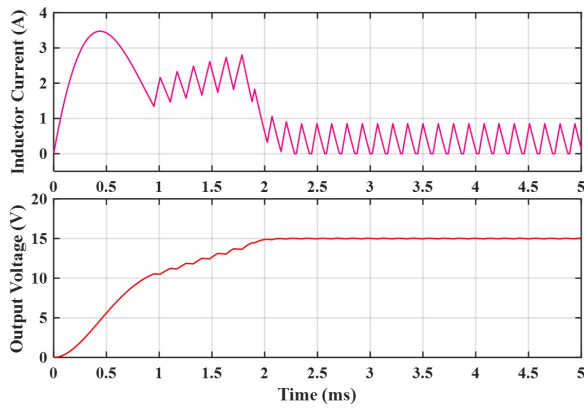


Fig. 3. Start-up (Time-triggered MPC)

Once the output voltage reaches the reference voltage, the inductor current decreases. With event-triggered MPC, once the converter reaches DCM, the number of event triggers

TABLE I
SIMULATION PARAMETERS

Converter and Controller Parameter	Value
Inductor (L)	$550\mu H$
Inductor DC Resistance (R_L)	1.3Ω
Output Capacitance (C)	$220\mu F$
Load Resistance (R)	73Ω
Sampling Period (T_s)	$5\mu s$
Prediction Horizon (N)	14
N_1	1
Move Blocking Coefficient (n_s)	4
Weight in Objective Function Lambda (λ)	0.5
δ	0.05
k_{max}	14

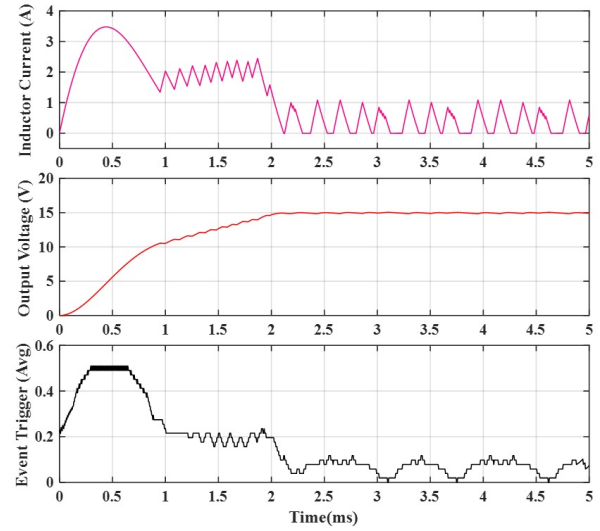


Fig. 4. Start-up (Event-Triggered MPC)

is significantly decreased as shown in Fig. 4. Using event-triggered MPC, we were able to achieve similar results while using significantly less computation.

B. Step Changes in the Output Reference Voltage

The performance of the converter with both time-triggered MPC and event-triggered MPC were evaluated when the output reference voltage was stepped up from 15V to 30V at 7.5ms. As can be seen from Figs 5 and 6, the output achieves a regulated 30V output at approximately 19ms for time-triggered MPC. The inductor current slightly increases during the step up in reference voltage to increase the output voltage. Once the converter reaches regulation, the inductor current is reduced. For event-triggered MPC, the converter reaches a regulated 30V output at approximately 21.5ms, a 2.5ms delay compared to time-triggered formulation. The converter's performance is almost equivalent for the two techniques, with the average number of computations significantly reduced with the latter method.

Next, the output voltage reference is changed from 20V to 15V at 10ms. The response of the converter using both

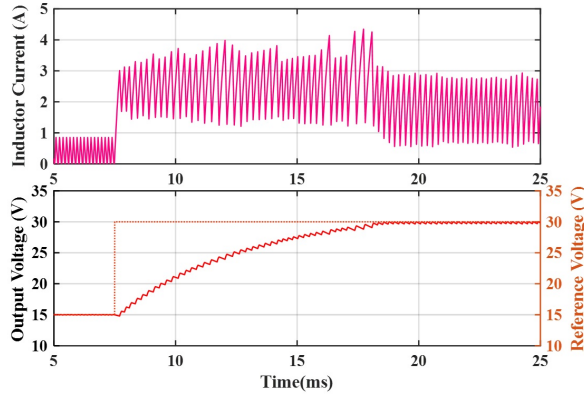


Fig. 5. Reference voltage step-up from 15V to 30V (Time-triggered MPC)

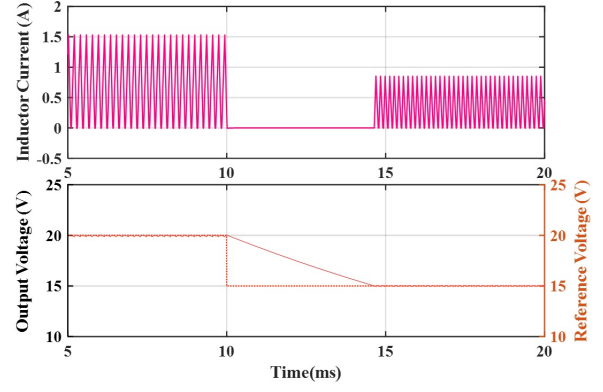


Fig. 7. Reference voltage step-down from 20V to 15V (Time-triggered MPC)

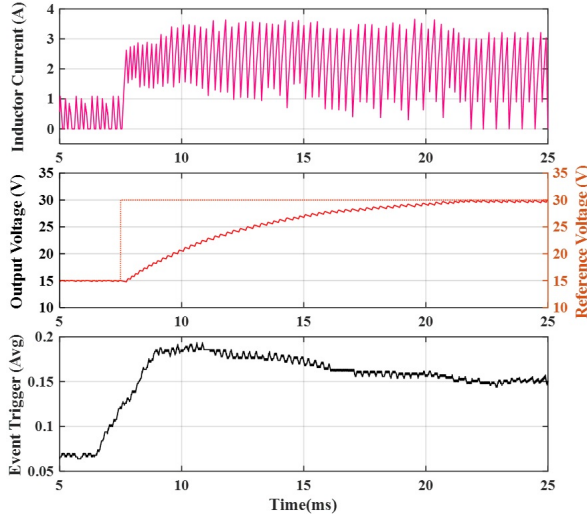


Fig. 6. Reference voltage step-up from 15V to 30V (Event-Triggered MPC)

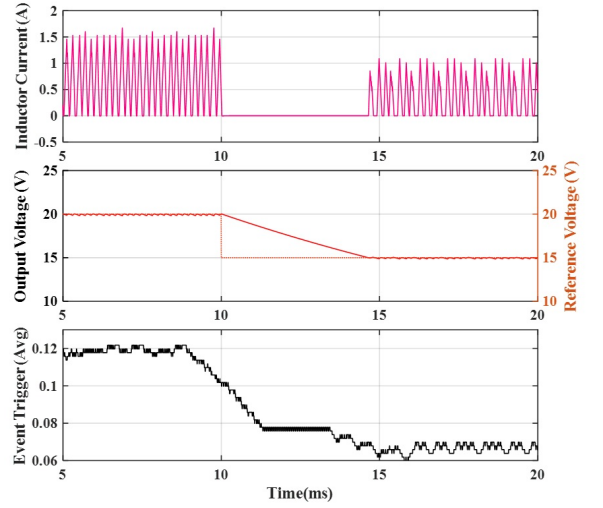


Fig. 8. Reference voltage step-down from 20V to 15V (Event-Triggered MPC)

time-triggered MPC and event-triggered MPC methods are illustrated in Figs 7 and 8. Both control methods allow the converter to reach regulation within 5ms with the latter achieving similar performance with significantly reduced calculations. During the step down in reference voltage, the inductor current goes to zero allowing the capacitor to discharge into the load to reduce the output voltage to the new reference voltage.

C. Step Change in the Input Voltage

In this case, a step change in the input voltage is simulated. More specifically, the input, v_s , is stepped up from 10V to 15V at 20ms after steady state operation with the reference voltage, v_{ref} , set to 30V. The line transient response of the converter for both methods is displayed in Figs 9 and 10. The output voltage remains almost undisturbed during the input transient. The number of event triggers decreases once the input increases to 15V. The plot did not include the start-up profile of the converter, but it was noted that the number of events continuously decreases as the converter approaches steady state. It does take the converter more time to reach 30V steady state using event-triggered control. The event-

triggered controlled converter reached steady state at 16ms while the time-triggered controlled converter reached steady state at 13ms.

D. Discussion of Computational Savings

Finally, the computational savings for all simulated cases are summarized in Table II, measured by the average event frequency. As can be seen, the proposed event-triggered MPC requires only 7% – 20% control effort as compared to time-triggered MPC, while maintaining comparable performance. Please note that the balancing between computation reduction and control performance can be achieved by calibrating the threshold parameter δ , and a thorough analysis of its impact is left as future work.

V. CONCLUSION

This paper investigates the use of event-triggered enumeration-based model predictive control (MPC) for DC-DC boost converter control. Specifically, event-triggered MPC is used to reduce the computational burden of conventional time-triggered MPC. Simulation results demon-

TABLE II
COMPUTATIONAL SAVING AS MEASURED BY EVENT FREQUENCY

Operation Modes (Conditions as listed in IV)	Average Computation
Start-up	20%
Steady state $v_s=10V$, $v_o=15V$	7%
Steady state $v_s=10V$, $v_o=20V$	12%
Steady state $v_s=10V$, $v_o=30V$	16%
Steady state $v_s=15V$, $v_o=15V$	14%
Step-up in reference voltage	19%
Step-down in reference voltage	8%
Step-up in input voltage	15%

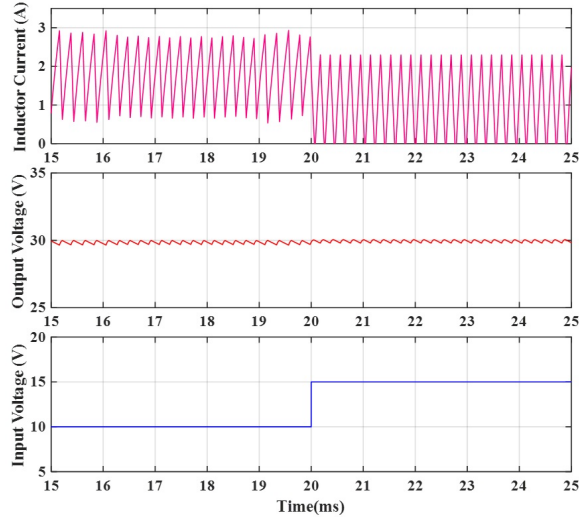


Fig. 9. Input voltage step-up from 10V to 15V (Time-triggered MPC)

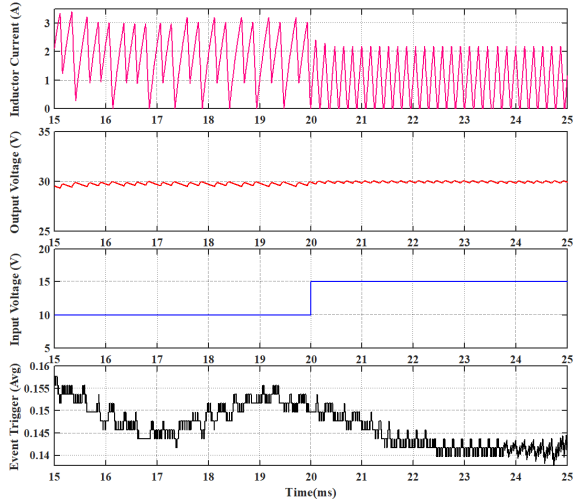


Fig. 10. Input voltage step-up from 10V to 15V (Event-Triggered MCP)

strate the effectiveness of the proposed methodology by reducing the average online computations by up to 93%, while maintaining a comparable control performance. Future work includes further developing the controller design to improve voltage regulation during output load excursions and to include current control. Investigating the impact of the threshold, δ , on stability and performance is another work direction. Furthermore, we will also focus on implementing the proposed control algorithms in hardware to verify the feasibility of real-time implementation.

REFERENCES

- [1] S. Kouro, P. Cortés, R. Vargas, U. Ammann, and J. Rodríguez, "Model predictive control—a simple and powerful method to control power converters," *IEEE Transactions on Industrial Electronics*, vol. 56, no. 6, pp. 1826–1838, 2008.
- [2] M. Saoudi, A. El-Sayed, and H. Metwally, "Design and implementation of closed-loop control system for buck converter using different techniques," *IEEE Aerospace and Electronic Systems Magazine*, vol. 32, no. 3, pp. 30–39, 2017.
- [3] M. S. Fadali and A. Visioli, *Digital control engineering: analysis and design*. Academic Press, 2013.
- [4] P. Karamanakos, T. Geyer, and S. Manias, "Direct voltage control of dc–dc boost converters using enumeration-based model predictive control," *IEEE Transactions on Power Electronics*, vol. 29, no. 2, pp. 968–978, 2013.
- [5] P. P. Karamanakos, "Model predictive control strategies for power electronics converters and ac drives," 2013.
- [6] Z. Leng and Q. Liu, "A simple model predictive control for buck converter operating in ccm," in *IEEE PRECEDE*, 2017, pp. 19–24.
- [7] F. A. Villarroel, J. R. Espinoza, M. A. Pérez, R. O. Ramírez, C. R. Baier, D. Sbárbaro, J. J. Silva, and M. A. Reyes, "Stable shortest horizon fcs-mpc output voltage control in non-minimum phase boost-type converters based on input-state linearization," *IEEE Transactions on Energy Conversion*, vol. 36, no. 2, pp. 1378–1391, 2021.
- [8] S. Huang and J. Chen, "Event-triggered model predictive control for autonomous vehicle with rear steering," *SAE Technical Paper*, no. 2022-01-0877, 2022.
- [9] J. Chen, X. Meng, and Z. Li, "Reinforcement learning-based event-triggered model predictive control for autonomous vehicle path following," in *2022 American Control Conference*, Atlanta, GA, June 8–10, 2022.
- [10] J. Yoo and K. H. Johansson, "Event-triggered model predictive control with a statistical learning," *IEEE Transactions on Systems, Man, and Cybernetics: Systems*, vol. 51, no. 4, pp. 2571–2581, 2021.
- [11] F. D. Brunner, W. Heemels, and F. Allgöwer, "Robust event-triggered MPC with guaranteed asymptotic bound and average sampling rate," *IEEE Trans. Autom. Control*, vol. 62, no. 11, pp. 5694–5709, 2017.
- [12] H. Li and Y. Shi, "Event-triggered robust model predictive control of continuous-time nonlinear systems," *Automatica*, vol. 50, no. 5, pp. 1507–1513, 2014.
- [13] A. Eqtami, D. V. Dimarogonas, and K. J. Kyriakopoulos, "Novel event-triggered strategies for model predictive controllers," in *2011 50th IEEE Conference on Decision and Control and European Control Conference*, Orlando, FL, December 12–15, 2011, pp. 3392–3397.
- [14] K. Hashimoto, S. Adachi, and D. V. Dimarogonas, "Self-triggered model predictive control for nonlinear input-affine dynamical systems via adaptive control samples selection," *IEEE Transactions on Automatic Control*, vol. 62, no. 1, pp. 177–189, 2016.
- [15] J. Chen and Z. Yi, "Comparison of event-triggered model predictive control for autonomous vehicle path tracking," in *IEEE Conf. Control Technology and Applications*, San Diego, CA, Aug. 8–11, 2021.
- [16] D. Lehmann, E. Henriksson, and K. H. Johansson, "Event-triggered model predictive control of discrete-time linear systems subject to disturbances," in *2013 European Control Conference (ECC)*. IEEE, 2013, pp. 1156–1161.